

# Systemic arterial pressure wave reflections during acute hemorrhage\*

Paul Dark, BSc, MB, PhD, FRCS; Rod Little, BSc, PhD, FRCPath; Mahesh Nirmalan, MD, PhD, FRCA; Jon Purdy, BSc, PhD

**Objective:** To determine the effects of hemorrhage on wave-reflection-induced systolic pressure augmentation in the aorta.

**Design:** Randomized, controlled laboratory experiment.

**Setting:** University research laboratory.

**Subjects:** Twenty-five anesthetized pigs randomized to surgical controls (n = 7), hemorrhage (n = 9, H), and hemorrhage with reinfusion (n = 9, HR).

**Interventions:** Hemorrhage of 1 mL/kg/min over 20 mins followed by observation (H) or reinfusion (HR) of shed blood.

**Measurements and Main Results:** High-fidelity systemic arterial pressure waveforms, from ascending aorta to femoral artery, were transduced and archived digitally using intravascular semi-conductor catheter-tipped pressure transducers. Wave-reflection-induced systolic pressure augmentation was determined using the augmentation index in the ascending aorta (AI<sub>aa</sub>) and distal descending aorta (AI<sub>da</sub>). Pulse wave velocity, wave travel times, and lumped pressure wave reflection sites were also calculated. AI values were positive at baseline with greater decreases in AI<sub>da</sub> compared with AI<sub>aa</sub> observed following hemorrhage, with negative values achieved for AI<sub>da</sub> alone. AI returned to control values following reinfusion. Lumped reflection site positions and pres-

sure contour maps suggested that a single lumped reflection site (lower abdomen/pelvis) at baseline was replaced by two discrete sites (upper abdomen and pelvis) following hemorrhage, which only recovered following reinfusion. Hemorrhage was associated with hemodynamic conditions that favored late return of wave reflection from the trunk and with the absence of significant changes in systemic vascular resistance.

**Conclusions:** Hemorrhage-induced early return of pressure wave reflection from the abdominal vasculature is associated with systolic pressure augmentation in the ascending aorta and has the potential to worsen afterload conditions and decrease coronary artery perfusion and cardiac performance. Hemorrhage-induced splanchnic vasoconstriction causing pressure wave reflection may explain these loading conditions in the ascending aorta, and systolic pressure augmentation may be a more useful guide to left ventricular afterload than systemic vascular resistance. (Crit Care Med 2006; 34:1497–1505)

**KEY WORDS:** blood pressure; pressure wave reflection; augmentation index; pulse wave velocity; ventricular afterload; hemorrhage

Our current understanding of integrative cardiovascular pathophysiology during critical illness is governed, largely, by a pragmatic assumption that the heart produces constant pressure and flow (e.g., mean arterial pressure in mm Hg and cardiac output in L/min). Indeed, this is the basis on which medicine is currently practiced. For example, the deriva-

tion of mean arterial pressure provides an important parameter in the definitions of severe sepsis and septic shock, with subsequent acute therapeutic interventions aimed at, in part, the restoration of mean pressure. However, the systemic arterial tree is a complex hydraulic system that conducts forward pulsatile pressure and flow waves that result from intermittent cardiac contraction (1, 2). Furthermore, pulse waves are reflected from within the arterial system at sites of distensibility change, at branch points, and, in particular, from high-resistance arterioles, resulting in the retrograde conduction of pressure waves back to the central circulation (3). The velocity of systemic arterial waves can allow reflection activity to return to the aorta during the same systolic period, augmenting peak systolic pressure and worsening left ventricular afterload conditions (4, 5). In addition, the spatial proximity of the regional vasoactive arterial beds in humans results

in wave superposition and a single reflected wave apparent within the proximal aorta (Fig. 1), so-called “lumped pressure wave reflection” (6). In humans, these phenomena have been studied in health and aging as well as in chronic cardiovascular diseases such as hypertension and heart failure. An evidence base indicates that pulse wave velocity and pressure wave reflection are important in determining cardiac performance and that treatment for chronic hypertension and heart failure may be more efficacious when considering these factors (1, 2).

Factors that have been implicated in determining the timing and magnitude of reflected pressure waves from the peripheral circulation to ascending aorta include the length of ventricular systole (influenced by heart rate and left ventricular stroke volume), pulse wave velocity (influenced by arterial stiffness and mean arterial pressure), and peripheral vascular tone (1, 2, 7, 8). Furthermore, re-

\*See also p. 1569.

From the Faculty of Medical and Human Sciences, University of Manchester, UK (PD, RL, MN); Intensive Care Medicine, Hope Hospital, Salford, UK (PD); Critical Care Medicine, Manchester Royal Infirmary, UK (MH); and Department of Computer Science, University of Hull, UK (JP).

Supported, in part, by the Medical Research Council UK (Program Grant, University of Manchester, GA003DZ) and MRC Clinical Training Fellowship (PD).

The authors have no financial interests to disclose.

Copyright © 2006 by the Society of Critical Care Medicine and Lippincott Williams & Wilkins

DOI: 10.1097/01.CCM.0000215451.26971.89

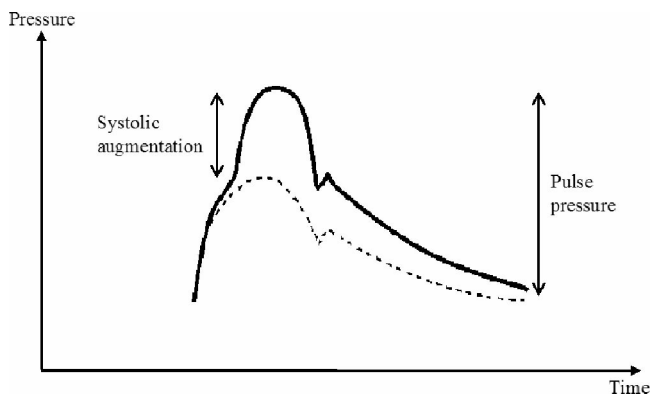


Figure 1. A blood pressure waveform recorded in the ascending aorta of an adult man during one heart period. The solid line is the recorded waveform, displaying systolic pressure wave augmentation, and the dashed line represents the predicted pressure waveform generated by the left ventricle in the absence of lumped pressure wave reflection. Augmentation index is the ratio of systolic augmentation to pulse pressure.

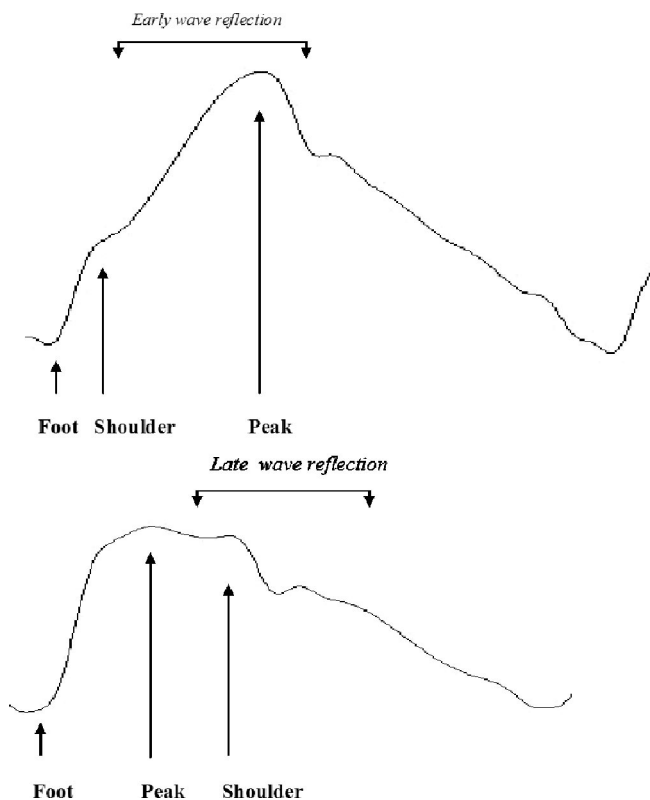


Figure 2. Examples of aortic pressure waveforms from the present study showing early and late wave reflection (arrows above waveforms) and the pertinent points for calculation of augmentation index (arrows below waveforms). Augmentation index was determined as the pressure difference from a shoulder to the peak divided by the pulse pressure (foot to peak difference). The upper waveform (an example of the ascending aorta at baseline) has a positive augmentation index (implying early reflection), and the lower (an example of the descending aorta following hemorrhage) has a negative index (implying late reflection). The timing of the reflected pressure wave in the lower waveform occurs around the time of the incisura.

gional peripheral vascular tone within the abdomen and trunk is thought to account for much of the pressure wave reflection activity throughout the systemic arterial system (9). When integrating these factors, pressure wave reflec-

tion returning to the proximal aorta can occur in systole (early return) or extend into diastole (late return) (Fig. 2) (8, 10, 11). Analogous to the effects of intra-aortic balloon counterpulsation, adolescents and young adults display a late re-

turning reflected pressure wave within the ascending aorta that does not augment systolic pressure, thereby limiting left ventricular afterload and promoting coronary artery filling (8). The converse is true for adults with increasing age and hypertension (10, 11), where increased aortic stiffness and pulse wave velocity favor the early return of reflected pressure waves. Children tend to display prominent systolic pressure augmentation (early return) probably because of their relatively short bodies (2).

Despite the accumulating evidence for the significance of systemic arterial pressure wave reflections and systolic pressure augmentation in chronic cardiovascular diseases, we can find no modern systematic studies that consider these phenomena in critical care. Therefore, in the present study, we aimed to investigate the effects of hemorrhage on pressure wave reflection within the systemic arterial system, the null hypothesis being that a controlled fixed volume hemorrhage does not effect systolic pressure augmentation within the aorta.

## MATERIALS AND METHODS

*Fixed Volume Hemorrhage and Reinfusion.* The present investigation was conducted with Home Office approval issued in conjunction with the Animal (Scientific Procedures) Act 1986, which conforms to the *Guide for the Care and Use of Laboratory Animals* published by the U.S. National Institutes of Health (12). Twenty-five immature female Large-White pigs (mean weight  $24.8 \pm 0.9$  kg) were anesthetized, mechanically ventilated, and surgically prepared for hemodynamic monitoring as described previously (13–15). An infusion of intravenous Saffan (alphaxalone and alphadolone acetate) at a rate of 15 mg/kg/hr was used for maintenance anesthesia, and intermittent positive pressure mechanical ventilation was performed to deliver an oxygen/nitrous oxide mix ( $F_{IO_2}$  0.5) and to maintain an end-tidal  $CO_2$  of 40 mm Hg as in previous studies (13–15). An intravenous infusion of 10 mL/kg/hr 0.9% sodium chloride was commenced during surgical preparation and discontinued at the start of the experimental protocol. A 1-hr rest period separated surgical preparation and the experimental protocol.

Following surgical preparation, the pigs were randomly assigned to one of three groups: surgical control (SC,  $n = 7$ ), hemorrhage alone (H,  $n = 9$ ), and hemorrhage followed by reinfusion of shed blood (HR,  $n = 9$ ). Hemorrhage was conducted at a rate of 1 mL/kg/min for 20 mins (27% estimated total blood volume loss) (16) via a cannula in the left axillary artery and controlled using a calibrated rotary pump (Smith & Nephew Watson

Marlow, UK). Shed blood was collected in empty sterile 1-L 0.9% sodium chloride bags that were pretreated with 1500 units of heparin (Monoparin, CP Pharmaceuticals, UK). Each bag was maintained at core body temperature for each animal using a heated water bath. Animals randomized to reinfusion received filtered blood (200  $\mu$  Blood Set, Baxter S.A. Belgium) at a rate of 1 mL/kg/min via the right external jugular vein. Three measurement periods were defined: the start of the experimental period (baseline), following the hemorrhage period (P1), and following the reinfusion period (P2). Each measurement phase included a 5-min rest period to allow hemodynamic stabilization and a further 10-min period for completion of all hemodynamic measurements and blood sampling. Core body temperature was controlled as described previously (14).

**High-Fidelity Arterial Pressure Waveform Transduction and Acquisition.** Three high-fidelity semiconductor catheter-tipped pressure transducers (Codman, Johnson and Johnson, UK) were used to monitor arterial pressure waveforms from ascending aorta to femoral artery with lateral transduction. One catheter was introduced through a surgical arteriotomy in the right axillary artery and advanced until a left ventricular pressure waveform was transduced. Positioning within the proximal ascending aorta was achieved by monitoring the characteristic pressure waveform changes during catheter withdrawal from the ventricle. The catheter was secured at the skin surface with sutures. A second catheter was introduced via an arteriotomy in the medial musculocutaneous artery of the right thigh, a branch of the superficial femoral artery in the pig. The catheter was advanced into the common femoral artery and the position confirmed using a transcutaneous Doppler ultrasound device (9044 Portable Doppler, Deltex Medical, Chichester, UK). The catheter was secured at the skin surface with sutures. Finally, a left femoral surgical arteriotomy was performed to introduce an 8.5-Fr polyurethane sheath (Baxter Healthcare, USA) to allow passage of a 6-Fr Fasguide angiography catheter (Boston Scientific, CA) preloaded with a semiconductor catheter-tipped pressure transducer that protruded 1 cm beyond the end of the Fasguide. The loaded Fasguide was advanced from femoral artery to aortic arch in measured 5-cm steps, allowing a cascade of pressure waveforms to be recorded. The default position of this third catheter was in the distal descending aorta, as determined by transesophageal Doppler ultrasonography (Cardio Q, Deltex Medical, Chichester, UK). Figure 3 summarizes these transducer positions. In a preliminary study we found that complete occlusion of the left femoral artery, right axillary artery, and left axillary artery, both in turn and in combination, did not change any of the recorded hemodynamic or vascular variables compared with baseline

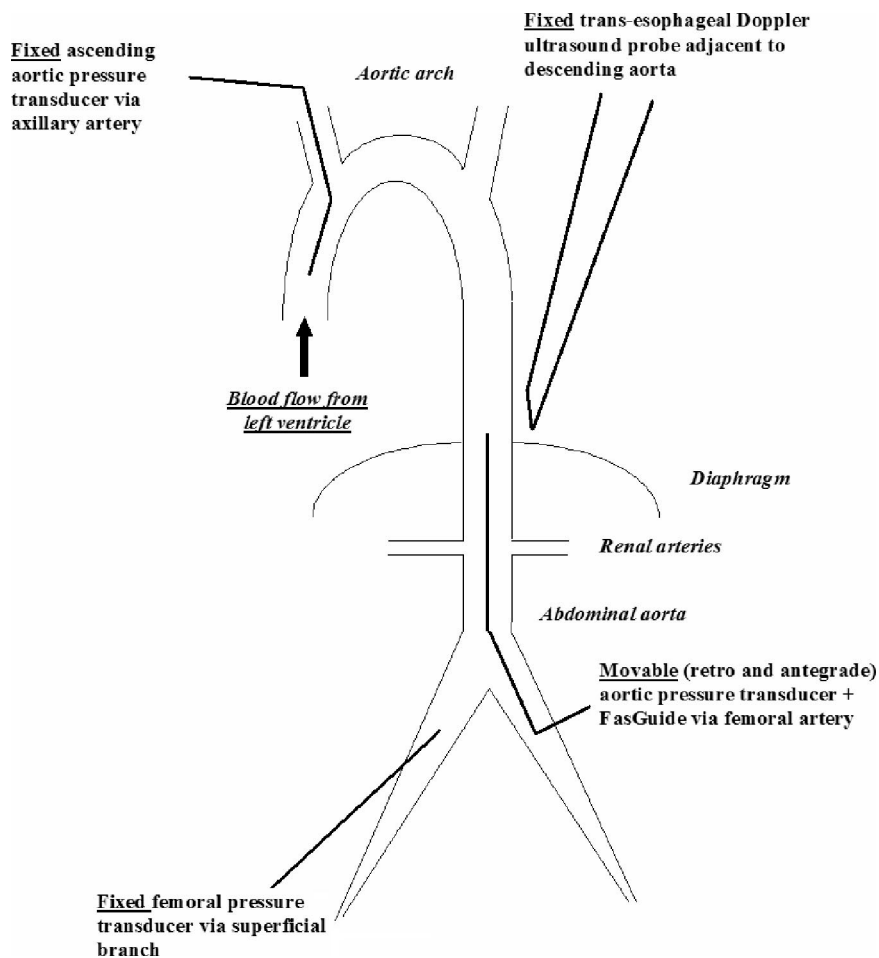


Figure 3. Schematic diagram of intravascular pressure transducer positions.

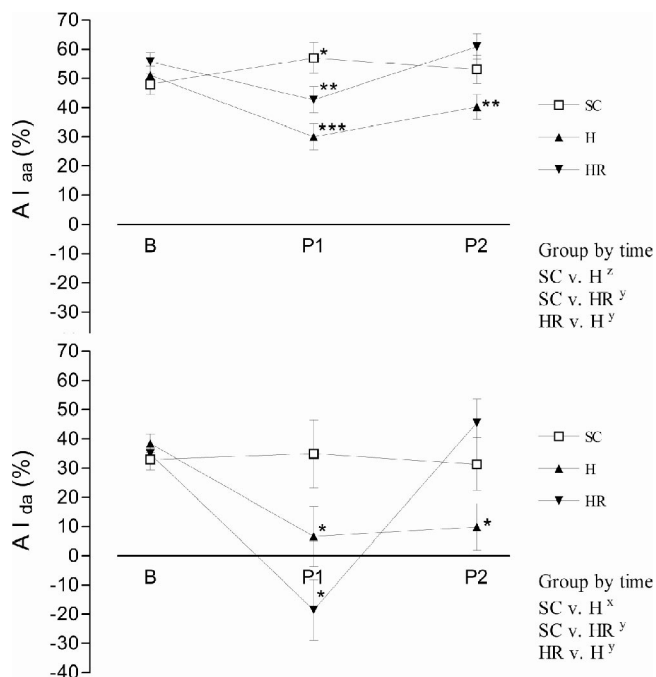


Figure 4. Ascending aortic ( $AI_{aa}$ ) and distal descending aortic ( $AI_{da}$ ) augmentation index responses to hemorrhage and autologous reinfusion (mean  $\pm$  SEM). Within-group differences compared with baseline, \* $p \leq .05$ , \*\* $p \leq .01$  and \*\*\* $p \leq .001$ . Group by time comparisons  $^x p \leq .05$ ,  $^y p \leq .01$ , and  $^z p \leq .001$ . Surgical control (SC), hemorrhage (H), and hemorrhage/reinfusion (HR) groups are shown at baseline (B), end of hemorrhage (P1), and end of reinfusion (P2).

(17). All experiments were conducted under terminal anesthesia. At autopsy, major aortic branches and catheter positions were confirmed and measured with respect to the ascending aorta.

The analog electrical output from each transducer was digitally converted using a multiple-channel data acquisition card (ADC27E, Amplicon, Brighton, UK) with 12-bit resolution. The digital pressure waveforms were displayed on a monitor in real time and archived simultaneously on compact disc. The phase of the mechanical ventilator cycle was recorded on compact disc alongside the pressure waveforms (17). The sample rate for each pressure channel was 1.6 kHz. Digital pressure was linear over the range 0–200 mm Hg compared with mercury manometry, and the dynamic responses were found to be flat in terms of frequency and phase to beyond 50 Hz (17). Each transducer was calibrated using a mercury manometer before each experiment and zero referenced to midchest.

During the measurement periods, simultaneous compact disc archives of systemic arterial waveforms were made from the ascending aorta, distal descending aorta, and left femoral artery over a continuous 20-sec period. Furthermore, 20-sec archives were made consecutively at every 5-cm position from aortic arch to right femoral artery using the catheter-loaded Fasguide arrangement.

**Signal Processing and Systolic Pressure Augmentation.** Signal processing was conducted off-line using our own purpose written software (Matlab 5.3, MathWorks, Natick, MA). Only pressure waveforms in end-expiration were analyzed. An individual pressure waveform within each data file was accepted only if the correlation function “corrcoef (x)” in Matlab 5.3 (18) was  $\geq 0.95$  when compared with a time averaged waveform from all of the end expiratory waveforms within the same file. This signal selection methodology excluded <5% of waveforms from end-expiration, usually because of ectopic beats (17). Subsequently, any parameters calculated from the accepted waveforms within a 20-sec data file ( $n = 6-8$ ) were summated and the means returned for further analysis. Time averaged cascade plots of pulse pressure waveform propagation from the aortic arch to femoral artery were constructed using the surface function in Matlab 5.3.

Augmentation index (AI) was used to determine wave reflection-induced systolic pressure augmentation in the aorta (8). AI was validated for this purpose during cardiac catheterization studies (8) but in recent years has been reported in numerous experimental and clinical studies. AI is a continuous variable that describes the ratio of the augmenting reflected pressure wave to total pulse pressure (Fig. 1). By convention, it takes positive values when augmenting the peak systolic pressure (early return of reflection), and negative values when it does not contribute to peak systole (late return of reflection) (Figs. 2). We devel-

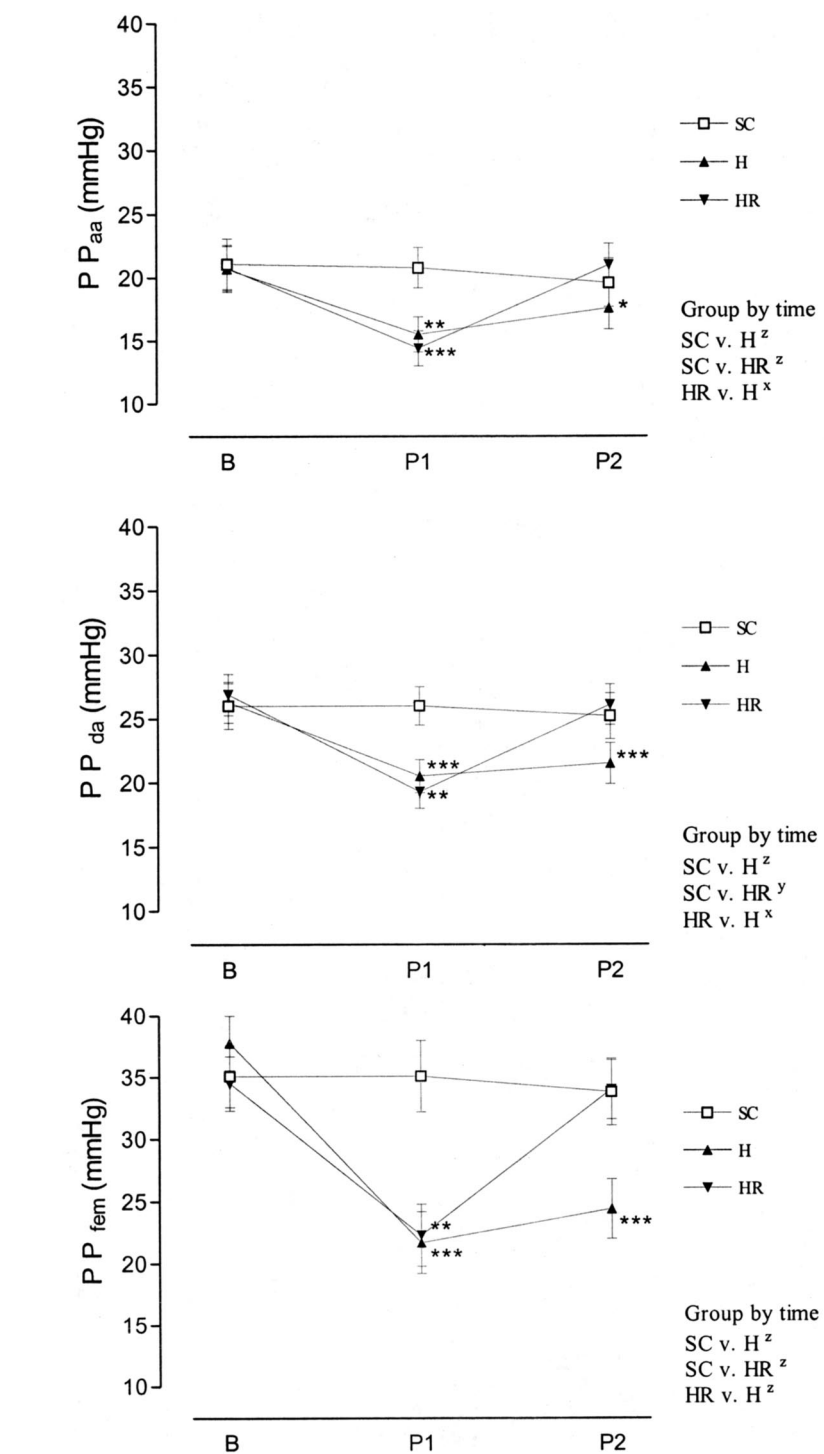


Figure 5. Pulse pressure responses in the ascending aorta ( $PP_{aa}$ ), distal descending aorta ( $PP_{da}$ ), and femoral artery ( $PP_{fem}$ ) to hemorrhage and autologous reinfusion (mean  $\pm$  SEM). Within-group differences compared with baseline: \* $p \leq .05$ , \*\* $p \leq .01$ , and \*\*\* $p \leq .001$ . Group by time comparisons  $^z p \leq .05$ ,  $^y p \leq .01$ , and  $^x p \leq .001$ . Surgical control (SC), hemorrhage (H), and hemorrhage/reinfusion (HR) groups are shown at baseline (B), end of hemorrhage (P1), and end of reinfusion (P2).

oped our own software to implement the signal processing method of Karamanoglu (19) to return the augmentation indices from pressure waveforms measured in the ascending aorta ( $AI_{aa}$ ) and the descending aorta ( $AI_{da}$ ). This approach depended on identifying shoul-

der points (Fig. 2) on the rising and/or falling edges of the pressure waveforms using the zero crossing of the fourth derivative of pressure with respect to time (2) and is described in detail elsewhere (17, 19). Femoral artery augmentation cannot be assessed because

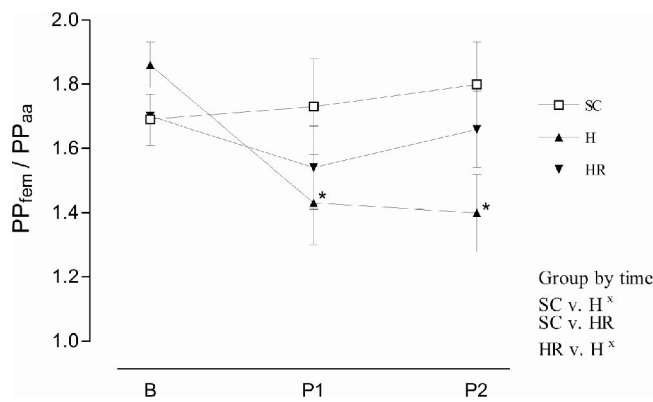


Figure 6. Pulse wave amplification (ascending aorta [ $PP_{aa}$ ] to femoral artery [ $PP_{fem}$ ]) responses to hemorrhage and autologous reinfusion (mean  $\pm$  SEM). Within-group differences compared with baseline: \* $p \leq .05$ , \*\* $p \leq .01$ , and \*\*\* $p \leq .001$ . Group by time comparisons \* $p \leq .05$ ,  $^y p \leq .01$ , and  $^z p \leq .001$ . Surgical control (SC), hemorrhage (H), and hemorrhage/reinfusion (HR) groups are shown at baseline (B), end of hemorrhage (P1), and end of reinfusion (P2).

Table 1. Wave travel times, pulse wave velocity, and lumped pressure wave reflection site responses to hemorrhage and autologous reinfusion (mean  $\pm$  SEM)

Group	B	P1	P2	Group by Time
Wave travel time ascending aorta, $10^{-3}$ sec				
SC	88 $\pm$ 5	87 $\pm$ 4	89 $\pm$ 7	SC vs. H <sup>a</sup>
H	85 $\pm$ 6	53 $\pm$ 8 <sup>b</sup>	63 $\pm$ 7 <sup>b</sup>	SC vs. HR <sup>a</sup>
HR	103 $\pm$ 9	65 $\pm$ 6 <sup>b</sup>	106 $\pm$ 8	HR vs. H <sup>a</sup>
Wave travel time descending aorta, $10^{-3}$ sec				
SC	74 $\pm$ 5	73 $\pm$ 4	68 $\pm$ 7	SC vs. H
H	67 $\pm$ 6	51 $\pm$ 8	56 $\pm$ 7	SC vs. HR
HR	77 $\pm$ 9	79 $\pm$ 6	84 $\pm$ 8	HR vs. H
Intra-thoracic aortic pulse wave velocity, m/sec				
SC	5.73 $\pm$ 0.35	5.98 $\pm$ 0.38	5.99 $\pm$ 0.37	SC vs. H
H	5.00 $\pm$ 0.31	5.17 $\pm$ 0.33	5.32 $\pm$ 0.33	SC vs. HR
HR	5.67 $\pm$ 0.31	5.65 $\pm$ 0.33	5.69 $\pm$ 0.33	HR vs. H
Intra-abdominal pulse wave velocity, m/sec				
SC	8.12 $\pm$ 0.44	8.69 $\pm$ 0.29	8.77 $\pm$ 0.28	SC vs. H
H	8.79 $\pm$ 0.39	8.07 $\pm$ 0.26 <sup>c</sup>	8.30 $\pm$ 0.25	SC vs. HR <sup>d</sup>
HR	8.56 $\pm$ 0.39	7.80 $\pm$ 0.26 <sup>c</sup>	8.87 $\pm$ 0.25	HR vs. H
Lumped reflection site from ascending aorta, m				
SC	0.31 $\pm$ 0.03	0.32 $\pm$ 0.02	0.33 $\pm$ 0.03	SC vs. H <sup>a</sup>
H	0.30 $\pm$ 0.03	0.18 $\pm$ 0.02 <sup>b</sup>	0.22 $\pm$ 0.03 <sup>b</sup>	SC vs. HR <sup>a</sup>
HR	0.38 $\pm$ 0.03	0.22 $\pm$ 0.02 <sup>b</sup>	0.40 $\pm$ 0.03	HR vs. H <sup>a</sup>
Lumped reflection site from distal descending aorta, m				
SC	0.29 $\pm$ 0.04	0.31 $\pm$ 0.05	0.29 $\pm$ 0.05	SC vs. H
H	0.29 $\pm$ 0.04	0.21 $\pm$ 0.04	0.23 $\pm$ 0.04	SC vs. HR
HR	0.33 $\pm$ 0.04	0.31 $\pm$ 0.04	0.37 $\pm$ 0.04	HR vs. H

Surgical control (SC), hemorrhage (H), and hemorrhage/reinfusion (HR) groups are shown at baseline (B), end of hemorrhage (P1), and end of reinfusion (P2).

<sup>a</sup> $p \leq .001$ , group by time comparison; <sup>b</sup> $p \leq .001$ , within-group difference compared with baseline; <sup>c</sup> $p \leq .05$ , within-group difference compared with baseline; <sup>d</sup> $p \leq .05$ , group by time comparison. Mean distances of distal descending aorta, renal arteries, aortic bifurcation and femoral artery sites from ascending aorta were 0.18 m, 0.34 m, 0.44 m, and 0.59 m, respectively.

waveform superposition in this region does not allow resolution in the time domain (20). Pulse pressure (mm Hg) was measured in the ascending aorta ( $PP_{aa}$ ), distal descending aorta

( $PP_{da}$ ), and right femoral artery ( $PP_{fem}$ ). Pulse wave amplification from ascending aorta to femoral artery was calculated as  $PP_{fem}/PP_{aa}$ . Pulse wave velocities (m/sec) were calculated

from ascending to distal descending aorta ( $PWV_{thorax}$ ) and from distal descending aorta to right femoral artery ( $PWV_{abdomen}$ ), using the wavefront method (21). Wave travel time ( $\Delta t$ ) is the time taken for a pulse wave to pass from a measurement site to the effective lumped reflection site and back. We developed our own software to implement the signal processing method of Karamanoglu (19) to determine the wave travel time from the pressure waveforms in the ascending and descending aorta. This approach depended on determining the time difference between the shoulder or peak of the pressure wave traveling away from the heart and the shoulder or peak of the returning reflected wave (Fig. 2) and is described in detail elsewhere (17, 19). The effective position of a lumped reflection site can be calculated from the product of pulse wave velocity within the arterial system beyond the measurement site and half the wave travel time (5, 8). Therefore, lumped reflection sites were calculated for the ascending aorta ( $L_{aa}$ ) and the distal descending aorta ( $L_{da}$ ). A lumped pressure wave reflection site represents the superposition of all reflection activity from the different reflection sites beyond the point of measurement (1, 2).

**Standard Hemodynamic and Oxygen Delivery Monitoring.** Standard invasive core temperature, hemodynamic, and oxygen delivery monitoring was performed as described previously by our group (14, 15).

**Statistical Analysis.** One-way analysis of variance was used to determine any between-group differences at baseline. Repeated-measures analysis of variance (two-way analysis of variance with repeated measures in one factor—time) was used to determine group by time interactions for continuous data and within-group differences compared with baseline. Where significant group by time interactions existed, Gabriel's test for *post hoc* comparisons was used to compare the three experimental groups. Where the same parameter was measured in different parts of the circulation simultaneously, "position" was added as a third factor to the repeated-measures strategy (group, time, and position) with repeated measures on two factors (time and position). All statistical calculations were performed with SPSS 11.5 (SPSS, Chicago, IL). All  $p$  values are two-sided with a threshold alpha of .05 used to assign significance. Results are reported as mean ( $\pm$ SEM).

## RESULTS

Augmentation index was greater in the ascending aorta compared with the distal descending aorta throughout the experiments ( $48.7 \pm 2.2\%$  v.  $24.0 \pm 3.7\%$ ,  $p \leq .001$ ; calculated from the main effects of position in the repeated measure strategy). Compared with baseline, augmentation index was reduced following hemorrhage in both the ascending

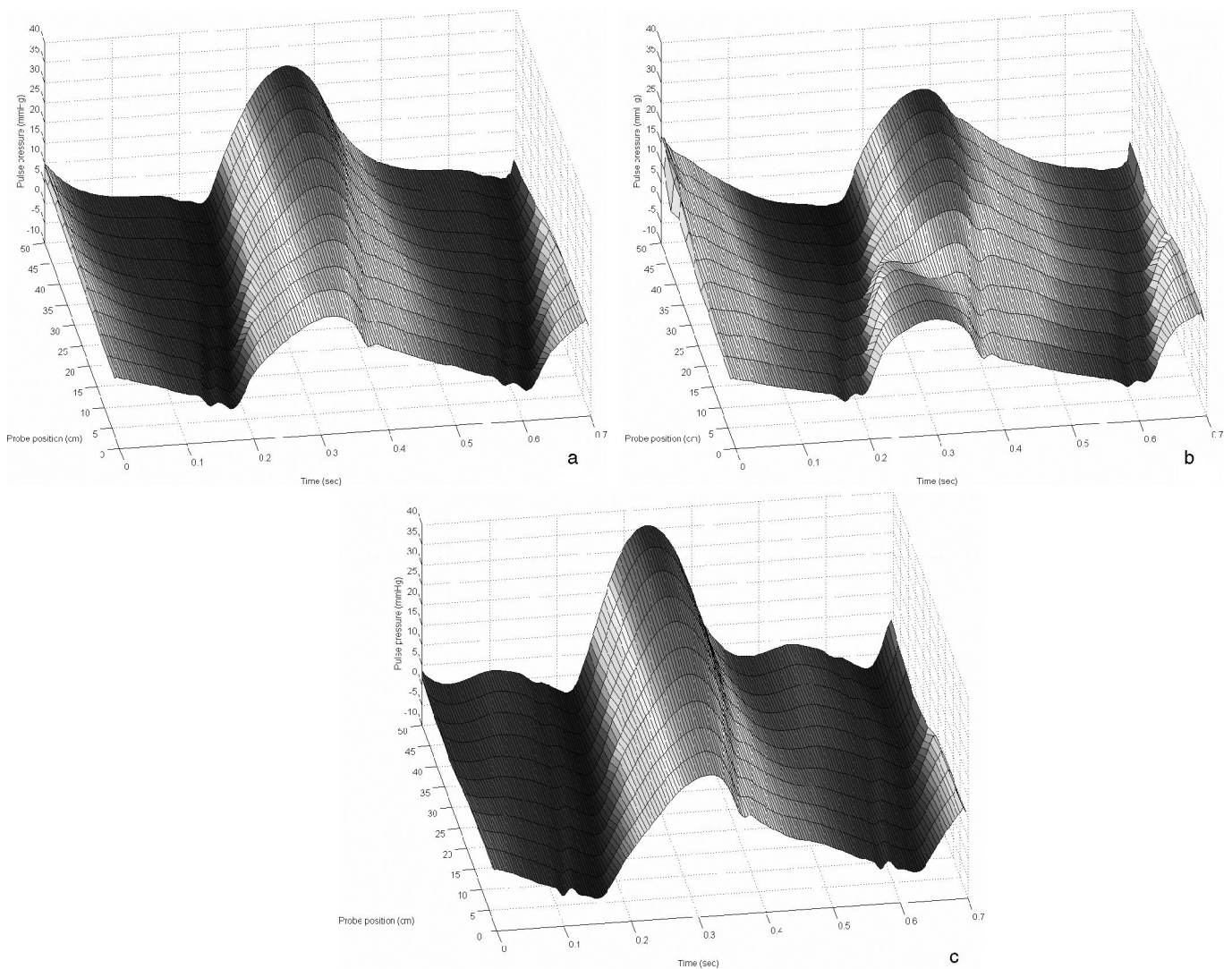


Figure 7. Examples of cascade plots of pulse pressure wave propagation from the same subject at baseline (a), following hemorrhage (b), and following reinfusion (c). Pressure probe positions are shown from aortic arch to femoral artery in 5-cm steps, with probe position indicated as distance (cm) from aortic arch.

and the distal descending aorta (Fig. 4). However, this pattern of change was more pronounced in the distal descending aorta with negative augmentation indices being achieved in half of the cases exposed to hemorrhage. A negative augmentation index was never achieved in the ascending aorta. Subsequent reinfusion resulted in recovery of the augmentation index at both sites to baseline values.

Hemorrhage resulted in a decrease in pulse pressure at each measurement site, with subsequent recovery following reinfusion (Fig. 5). Although these patterns of response were noted at each measurement site, they were more pronounced in the femoral artery. Systolic blood pressure decreases were greater than those of diastolic, explaining the decreases in pulse pressure following hemorrhage

( $-17 \pm 4$  mm Hg systolic pressure decrease vs.  $-13 \pm 4$  mm Hg diastolic pressure decrease in the ascending aorta,  $p < .001$  paired samples Student's  $t$ -test;  $-17 \pm 4$  vs.  $-11 \pm 4$  mm Hg in the distal descending aorta,  $p < .001$ ; and  $-23 \pm 5$  vs.  $-13 \pm 4$  mm Hg in the femoral artery,  $p < .001$ ). At baseline, the mean pulse wave amplification from ascending aorta to femoral artery was 1.75. Hemorrhage was associated with decreases in pulse wave amplification, which only recovered following reinfusion (Fig. 6).

At baseline, the mean lumped pressure wave reflection site, as seen from the ascending aorta, was just above the mean level of the renal arteries in all groups (Table 1). The mean lumped reflection site, as seen from the distal descending aorta, was within the pelvis. As seen from the ascending aorta, the site of lumped

pressure wave reflection drew closer, into the upper abdomen, following hemorrhage and recovered to baseline values following subsequent reinfusion (Table 1). If blood was not reinfused following hemorrhage, the lumped reflection site remained closer to the ascending aorta than baseline values. No significant pattern changes were seen over the course of the experiments for the lumped reflection sites when seen from the distal descending aorta.

Cascade plots of pulse pressure waveform propagation from the aortic arch to femoral artery provided a useful visualization of the results described previously. An example of a cascade plot is shown in Figure 7.

Standard systemic hemodynamic, oxygen delivery, and metabolic responses to

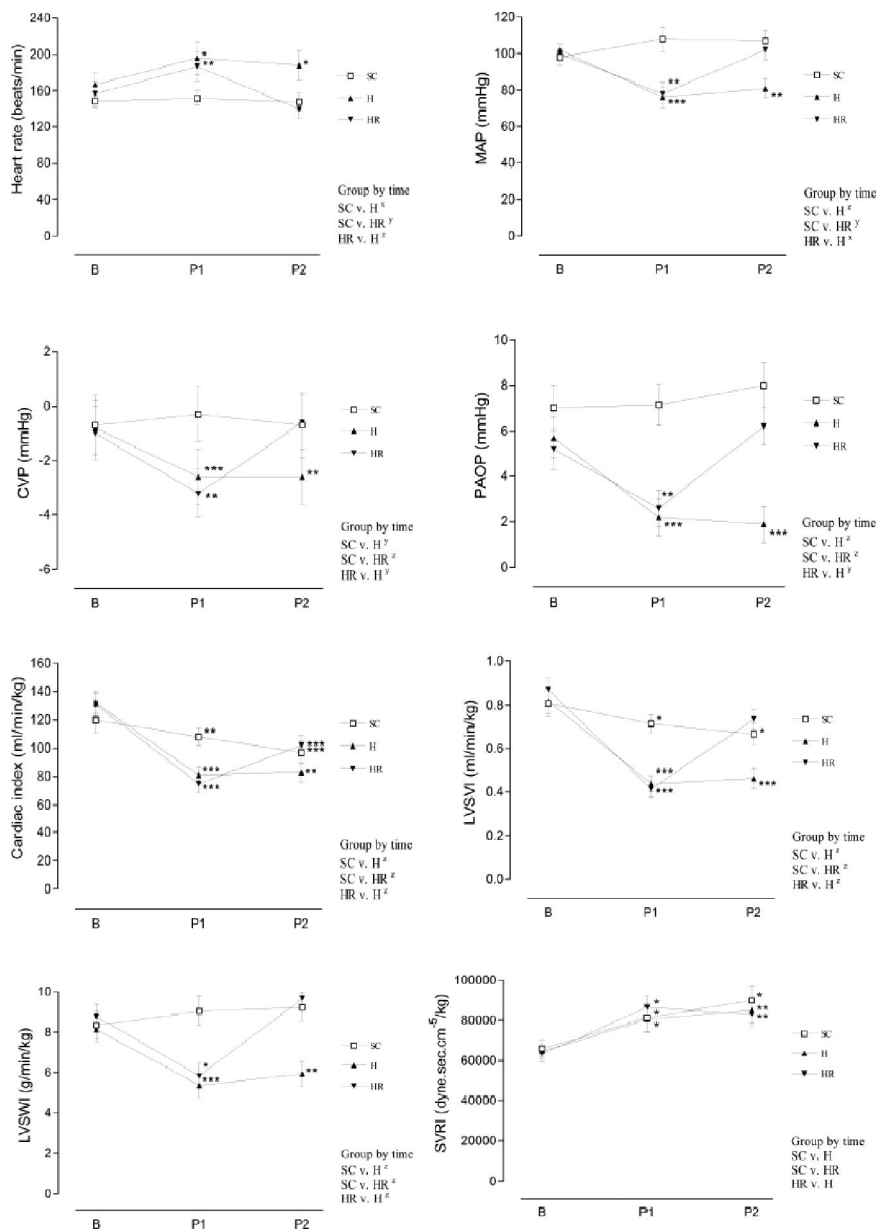


Figure 8. Standard hemodynamic responses to hemorrhage and autologous reinfusion (means  $\pm$  SEM). Within-group differences compared with baseline: \* $p \leq .05$ , \*\* $p \leq .01$ , and \*\*\* $p \leq .001$ . Group by time comparisons  $^y p \leq .05$ ,  $^z p \leq .01$ , and  $^z p \leq .001$ . Surgical control (SC), hemorrhage (H), and hemorrhage/reinfusion (HR) groups are shown at baseline (B), end of hemorrhage (P1), and end of reinfusion (P2). CVP, central venous pressure; LVSWI, left ventricular stroke work index; MAP, mean arterial pressure; PAOP, pulmonary artery occlusion pressure; LVSVI, left ventricular stroke volume index; SVRI, systemic vascular resistance index.

hemorrhage and reinfusion are shown in Figure 8 and Table 2.

## DISCUSSION

We found that anesthetized, ventilated, immature pigs displayed features of lumped pressure wave reflection as evidenced by positive (early) systolic augmentation in both the ascending and descending aorta at baseline. Furthermore, systolic augmentation was greater in the

ascending compared with the descending aorta, and positive pulse wave amplification (ascending aorta to femoral artery) was present at baseline. These findings are identical to pulse pressure waveform characteristics in immature humans (1, 2) and provide the first evidence for the importance of our porcine model in this type of integrative cardiovascular research.

Calculations of lumped reflection site positions at baseline were consistent with

other mammals, including humans (1, 2, 5, 8), where reflection sites in the lower abdomen and trunk predominate. Hemorrhage was associated with the development of an apparent uncoupling of lumped pressure wave reflection into two discrete sites: one around the upper abdomen, which was associated with the maintenance of early pressure wave reflection in the ascending aorta, and the other within the pelvis region associated with late returning pressure wave reflection in the descending aorta (Fig. 7). To our knowledge, this uncoupling phenomenon has not been described previously.

The uncoupling phenomenon was apparent in half of the 18 pigs exposed to hemorrhage, and the augmentation index responses in the aorta were normally distributed. Using multiple linear regression, we found that 53% of the variability in augmentation index in the descending aorta could be explained by a model of heart rate, mean arterial pressure, left ventricular stroke volume, systemic vascular resistance index, and abdominal pulse wave velocity (R value for the model of .73,  $p < 0.001$ ). Stepwise removal of systemic vascular resistance and abdominal pulse wave velocity did not change the model summary, and the remaining regression coefficients are shown in Table 3. These findings show that lumped pressure wave reflection uncoupling (i.e., the development of a negative augmentation index in the descending aorta in the present study) was associated with the lowest mean arterial pressures and left ventricular stroke volumes and the highest pulse rates in response to moderate hemorrhage. These results suggest that if we had continued our progressive hemorrhage a little further, we may have resolved pressure wave reflection uncoupling in the majority of pigs; although, with a severe hemorrhage (beyond 40% in our model), a depressor reflex eventually predominates causing precipitous cardiovascular collapse with bradycardia and severe vasodilation (22).

During hemorrhage, the development of late return pressure wave reflection from the lower body to the aorta was associated with the development of negative systolic pressure augmentation. When these hemodynamic circumstances develop in the proximal aorta, there can be associated improvements in left ventricular afterload, coronary artery perfusion, and cardiac performance akin to the effects of intra-aortic balloon counterpulsation (1, 2), a potentially favorable con-

**Table 2.** Standard systemic oxygen transport and metabolic responses to hemorrhage and autologous re-infusion (means  $\pm$  SEM)

Group	B	P1	P2	Group by Time
Mixed venous oxygen saturation, %				
SC	66.7 $\pm$ 1.4	64.3 $\pm$ 2.6	60.9 $\pm$ 2.3 <sup>a</sup>	SC vs. H <sup>c</sup>
H	69.3 $\pm$ 1.3	46.1 $\pm$ 2.3 <sup>c</sup>	46.7 $\pm$ 2.0 <sup>c</sup>	SC vs. HR <sup>c</sup>
HR	71.1 $\pm$ 1.3	47.1 $\pm$ 2.3 <sup>c</sup>	64.3 $\pm$ 2.0 <sup>b</sup>	HR vs. H <sup>c</sup>
Oxygen delivery index, mL/min/kg				
SC	17.0 $\pm$ 0.6	15.5 $\pm$ 0.8 <sup>a</sup>	14.0 $\pm$ 0.7 <sup>c</sup>	SC vs. H <sup>c</sup>
H	19.2 $\pm$ 1.5	11.1 $\pm$ 1.0 <sup>c</sup>	10.7 $\pm$ 0.7 <sup>c</sup>	SC vs. HR <sup>c</sup>
HR	19.3 $\pm$ 0.9	10.3 $\pm$ 0.8 <sup>c</sup>	15.3 $\pm$ 1.2 <sup>c</sup>	HR vs. H <sup>c</sup>
Oxygen consumption index, mL/min/kg				
SC	5.8 $\pm$ 0.4	5.5 $\pm$ 0.3	5.4 $\pm$ 0.3	SC vs. H
H	5.8 $\pm$ 0.3	5.9 $\pm$ 0.3	5.6 $\pm$ 0.3	SC vs. HR
HR	5.6 $\pm$ 0.3	5.3 $\pm$ 0.3	5.3 $\pm$ 0.3	HR vs. H
Oxygen extraction ratio				
SC	0.35 $\pm$ 0.01	0.37 $\pm$ 0.02	0.40 $\pm$ 0.02 <sup>a</sup>	SC vs. H <sup>c</sup>
H	0.32 $\pm$ 0.01	0.55 $\pm$ 0.02 <sup>c</sup>	0.55 $\pm$ 0.02 <sup>c</sup>	SC vs. HR <sup>c</sup>
HR	0.30 $\pm$ 0.01	0.54 $\pm$ 0.02 <sup>c</sup>	0.37 $\pm$ 0.02 <sup>b</sup>	HR vs. H <sup>c</sup>
Arterial pH				
SC	7.44 $\pm$ 0.1	7.45 $\pm$ 0.1	7.45 $\pm$ 0.1	SC vs. H
H	7.46 $\pm$ 0.1	7.47 $\pm$ 0.1	7.47 $\pm$ 0.1	SC vs. HR
HR	7.44 $\pm$ 0.1	7.45 $\pm$ 0.1	7.44 $\pm$ 0.1	HR vs. H
Arterial bicarbonate, mmol/L				
SC	28.1 $\pm$ 0.6	28.0 $\pm$ 0.6	27.8 $\pm$ 0.5	SC vs. H
H	28.4 $\pm$ 0.5	28.5 $\pm$ 0.5	28.5 $\pm$ 0.4	SC vs. HR
HR	27.9 $\pm$ 0.6	27.3 $\pm$ 0.5	27.7 $\pm$ 0.5	HR vs. H
Arterial base excess, mmol/L				
SC	4.0 $\pm$ 0.6	3.9 $\pm$ 0.5	3.9 $\pm$ 0.5	SC vs. H
H	4.5 $\pm$ 0.5	4.8 $\pm$ 0.5	4.8 $\pm$ 0.4	SC vs. HR
HR	3.8 $\pm$ 0.5	3.5 $\pm$ 0.5	3.6 $\pm$ 0.5	HR vs. H

Surgical control (SC), hemorrhage (H), and hemorrhage/reinfusion (HR) groups are shown at baseline (B), end of hemorrhage (P1), and end of reinfusion (P2).

Within group differences compared with baseline <sup>a</sup> $p \leq .05$ , <sup>b</sup> $p \leq .01$  and <sup>c</sup> $p \leq .001$ . Group by time comparisons <sup>z</sup> $p \leq .001$ .

**Table 3.** Linear regression coefficients for associations between the main explanatory variables and augmentation index in the descending aorta

	Unstandardized Regression Coefficients $\pm$ SEM	Standardized Regression Coefficients	Significance $p$
Left ventricular stroke volume index, mL/min/kg	35.2 $\pm$ 17.3	0.256	.045
Mean arterial pressure, mm Hg	0.50 $\pm$ 0.02	0.310	.002
Heart rate, beats/min	-0.27 $\pm$ 0.08	-0.383	.001

Unstandardized regression coefficients are in units of augmentation (%) per unit change in explanatory variable. The standardized coefficients allow a comparison between the explanatory variables.

sequence of hemorrhage. However, in our study, these changes in wave reflection from the lower body were masked by the development of early pressure wave reflection from a more proximal site, with associated positive systolic pressure augmentation in the ascending aorta. Augmented systolic pressure in the ascending aorta is associated with increased left ventricular afterload and decreased coronary artery perfusion and cardiac

performance (1, 2), a potentially detrimental consequence of hemorrhage.

Evidence for changes in systemic pressure wave reflection during hemorrhagic shock exists from studies around the time of World War II (23–26). These experiments involved fully grown dogs and, along with subsequent work on the hypotensive phase of the Valsalva maneuver in humans (27), showed that any stimulus with the potential to shorten ventricular systole, lower pulse wave velocity, and

increase peripheral vascular tone will be associated with prominent reflected waves returning to the central aorta much later in systole or into diastole, improving left ventricular afterload conditions. Hamilton (25) suggested that the presence of such pulse contour changes following hemorrhage may represent compensatory vasoconstriction. Our model is of moderate hemorrhage in immature pigs without evidence of inadequate tissue perfusion (shock), making direct comparison with studies of hemorrhagic shock in mature dogs rather difficult, particularly now it has been recognized that, uniquely, dogs are predisposed to concealed gastrointestinal hemorrhage and associated ischemia/infarction during hemorrhagic shock (28). However, our results do have some resonance with this literature; our hemorrhage model was associated with a later return of reflected pressure waves from the trunk to the central aorta (as a consequence of lower mean arterial pressure and intra-abdominal pulse wave velocity) and a relative shortening of ventricular systole (as a consequence of lower left ventricular stroke volume and higher pulse rate). The presence of the uncoupling phenomenon is not obvious in previous studies, although when blood pressure waveforms were recorded with the available instrumentation in historical experiments, ascending aortic contours were usually reported and not the distal descending aorta, where we discovered evidence for uncoupling.

Our results rely on the careful measurement and analysis of systemic arterial blood pressure waveforms. Traditionally, harmonic analysis of simultaneously recorded aortic pressure and velocity waveforms allows the derivation of complex vascular impedance as a measure of afterload and aids in the assessment of both the magnitude and the site of wave reflection activity within an elastic vessel (1, 2). However, with the high pulse rates encountered following hemorrhage in the present study, harmonic analysis returns few pertinent data points and makes interpretation of complex vascular impedance subject to considerable error (1). Emerging techniques of pressure and velocity analysis, not dependent on harmonic analysis, could prove more promising (29). We suggest that future comparative studies will help determine the optimal analytical approaches for use in critical care, where cardiovascular status can change rapidly and to extremes, and

that analyses based on pressure-velocity data should help clarify the findings reported here.

Systemic vascular resistance index (SVRI) responses to hemorrhage compared with surgical controls were rather unremarkable. This is perhaps surprising given that splanchnic vasoconstriction is part of the reflex homeostatic responses to a progressive hemorrhage (22, 30). However, the absence of SVRI responses is a common finding following hemorrhage (13, 15, 22, 30), and it is questionable whether this parameter of resistance, derived from global systemic mean arterial blood pressure and flow, adequately informs us about regional changes in vasoactive state (31). Splanchnic vasomotor tone is also thought to be important in determining systolic pressure augmentation in the proximal aorta (9). Therefore, although no independent measure of splanchnic vasomotor state was recorded in these experiments, it is possible that the development of lumped pressure wave reflection uncoupling in our model was related, in part, to the presence of splanchnic vasoconstriction within the abdominal compartment (Fig. 7) despite the absence of significant SVRI changes. The implication of our findings is that knowledge of systolic pressure wave augmentation in the ascending aorta may be more important than SVRI in understanding the potential for adverse ventricular afterload conditions following hemorrhage. Extending this concept further in critical care, we can see how the use of SVRI as a guide for vasopressor therapy in, for example, septic shock could lead to therapeutic misadventure in terms of ventricular afterload, coronary artery perfusion, and cardiac performance.

## CONCLUSIONS

Hemorrhage-induced early return of pressure wave reflection from the abdominal vasculature is associated with systolic pressure augmentation in the ascending aorta, which has the potential to worsen left ventricular afterload conditions and decrease coronary artery perfusion and cardiac performance. Hemorrhage-induced splanchnic vasoconstriction causing pressure wave reflection may explain these loading conditions in the ascending aorta, and systolic pressure augmentation may be

a more useful guide to left ventricular afterload than systemic vascular resistance.

## REFERENCES

1. Milnor WR: Hemodynamics. Second Edition. Baltimore, Williams & Wilkins, 1989
2. Nichols WN, O'Rourke MF: McDonalds Blood Flow in Arteries: Theoretical, Experimental and Clinical Principles. Fourth Edition. London, Arnold, 1998
3. Westerhof N, Sipkema P, van den Bos GC, et al: Forward and backward waves in the arterial system. *Cardiovasc Res* 1972; 6:648–656
4. Milnor WR: Arterial impedance as ventricular afterload. *Circ Res* 1975; 36:565–570
5. Latham RD, Westerhof N, Sipkema P, et al: Regional wave travel and reflections along the human aorta: A study with six simultaneous micromanometric pressures. *Circulation* 1985; 72:1257–1269
6. O'Rourke MF: Vascular impedance in studies of arterial and cardiac function. *Physiol Rev* 1982; 62:570–623
7. Wilkinson IB, MacCallum H, Flint L, et al: The influence of heart rate on augmentation index and central arterial pressure in humans. *J Physiol* 2000; 525:263–270
8. Murgu JP, Westerhof N, Giolma JP, et al: Aortic input impedance in normal man: Relationship to pressure wave forms. *Circulation* 1980; 62:105–116
9. Karamanoglu M, Gallagher DE, Avolio AP, et al: Functional origin of reflected pressure waves in a multibranched model of the human arterial system. *Am J Physiol* 1994; 267: H1681–H1688
10. Kelly R, Hayward C, Avolio A, et al: Noninvasive determination of age-related changes in the human arterial pulse. *Circulation* 1989; 80:1652–1659
11. Nichols WW, Nicolini FA, Pepine CJ: Determinants of isolated systolic hypertension in the elderly. *J Hypertens Suppl* 1992; 10: S73–S77
12. U.S. National Institutes of Health: Guide for Care and Use of Laboratory Animals. Bethesda, MD, National Institutes of Health, 1996
13. Mackway-Jones K, Foex BA, Kirkman E, et al: Modification of the cardiovascular response to hemorrhage by somatic afferent nerve stimulation with special reference to gut and skeletal muscle blood flow. *J Trauma* 1999; 47:481–485
14. Girolami A, Little RA, Foex BA, et al: Hemodynamic responses to fluid resuscitation after blunt trauma. *Crit Care Med* 2002; 30: 385–392
15. Foex BA, Kirkman E, Little RA: Injury modifies the hemodynamic and metabolic responses to hemorrhage in immature swine. *Crit Care Med* 2004; 32:740–746
16. Dingley J, Foex BA, Swart M, et al: Blood volume determination by the carbon monoxide method using a new delivery system: Accuracy in critically ill humans and precision in an animal model. *Crit Care Med* 1999; 27:2435–2441
17. Dark PM: Pulsatile Characteristics of the Systemic Arterial System During Acute Haemorrhagic Hypovolaemia [dissertation]. Manchester, UK, University of Manchester, 2002
18. Hanselman D, Littlefield B: Mastering Matlab 5: A Comprehensive Tutorial and Reference. Englewood Cliffs, NJ, Prentice Hall, 1998
19. Karamanoglu M: A system for analysis of arterial blood pressure waveforms in humans. *Comput Biomed Res* 1997; 30:244–255
20. O'Rourke M, Taylor MG: Vascular impedance of the femoral bed. *Circulation Research* 1966; 18:129–139
21. Pruet JD, Bourland JD, Geddes LA: Measurement of pulse-wave velocity using a beat-sampling technique. *Ann Biomed Eng* 1988; 16:341–347
22. Little RA, Kirkman E: Cardiovascular control after injury. In: Scientific Foundations of Trauma. Dudley HF, Cooper G, Gann DS, et al (Eds). Oxford, UK, Butterworth/Heinemann, 1997, pp 551–563
23. Wiggers CJ: The Pressure Pulses in the Cardiovascular System. London, Longman, 1928
24. Hamilton WF, Dow P: An experimental study of the standing waves in the pulse propagated through the aorta. *Am J Physiol* 1939; 125: 48–59
25. Hamilton WF: The patterns of arterial pressure pulse. *Am J Physiol* 1944; 141:235–241
26. Remington JW, Hamilton WF, Caddell MH, et al: Some circulatory responses to hemorrhage in dogs. *Am J Physiol*; 1950; 161: 106–115
27. Kroeker EJ, Wood EH: Beat-to-beat alterations in relationship of simultaneously recorded central and peripheral arterial pressure pulses during Valsalva maneuver and prolonged expiration in man. *J Appl Physiol* 1956; 8:483–494
28. Little RA, Foex BA: Animal models in critical care research. In: Current Topics in Intensive Care. Dellinger RP, Burchardi H, Dobb GJ, et al (Eds). London, Saunders, 1996 pp 148–165
29. Bleasdale RA, Parker KH, Jones CJH: Chasing the wave. Unfashionable but important new concepts in arterial wave travel. *Am J Physiol* 2003; 284:H1879–H1885
30. Scher N, Pawelczyk J, Ludbrook J: Blood Loss and Shock. London, Edward Arnold, 1994
31. Pinsky MR: Hemodynamic profile interpretation. In: Principles and Practice of Intensive Care Monitoring. Tobin MJ (Ed). New York, McGraw-Hill, 1999, pp 871–888